Korean J. Limnol. 41 (2) : 247~263 (2008)

Application of CE-QUAL-W2 [v3.2] to Andong Reservoir: Part I: Simulations of Hydro-thermal Dynamics, Dissolved Oxygen and Density Current

Bhattarai, Prasid Ram, Yoonhee Kim and Woomyoung Heo*

(Department of Environmental Disaster Prevention Engineering, Kangwon National University, Samcheok 245-711, Korea)

A two-dimensional (2D) reservoir hydrodynamics and water quality model, CE-QUAL-W2, is employed to simulate the hydrothermal behavior and density current regime in Andong Reservoir. Observed data used for model forcing and calibration includes: surface water level, water temperature, dissolved oxygen and suspended solids concentration. The model was calibrated to the year of 2003 and verified with continuous run from 2000 till 2004. Without major adjustments, the model accurately simulated surface water levels including the events of large storm. Deep-water reservoirs, like Andong Reservoir, located in the Asian Monsoon region begin to stratify in summer and overturn in fall. This mixing pattern as well as the descending thermocline, onset and duration of stratification and timing of turnover phenomenon were well reproduced by the Andong Model. The temperature field and distinct thermocline are simulated to within 2°C of observed data. The model performed well in simulating not only the dissolved oxygen profiles but also the metalimnetic dissolved minima phenomenon, a commonly occurring phenomenon in deep reservoirs of temperate regions. The Root Mean Square Error (RMSE) values of model calibration for surface water elevation, temperature and dissolved oxygen were 0.0095 m, 1.82°C, and 1.13 mg L^{-1}, respectively. The turbid storm runoff, during the summer monsoon, formed an intermediate layer of about 15 m thickness, moved along the metalimnion until being finally discharged from the dam. This mode of transport of density current, a common characteristic of various other large reservoirs in the Asian summer monsoon region, was well tracked by the model.

Key words : hydro-thermal dynamics, metalimnetic DO minima, turbid interflow, CE-QUAL-W2

INTRODUCTION

Nakdong River, the longest river in Korea (river length of 521.5 km), serves as an important water resource for the south eastern areas. Located in North Kyoungsang province, Andong Reservoir (Fig. 1) is in the most upstream chain of major reservoirs on the Nakdong River system.

Andong Reservoir, an earth rock-filled dam standing 83 m high and 612 m long, was completed in 1977. This multi-purpose reservoir is operated by Korea Water Resource Corporation (hereafter KWATER) with the main functions of flood control (110 million m^3), water supply (a total of 926 million m^3 for industrial, agricultural and municipal purposes), and generation of hydroelectric power (158 GWh) (KWATER, 2006).

* Corresponding author: Tel: 033) 570-6573, Fax: 033) 574-7262, E-mail: woo@kangwon.ac.kr

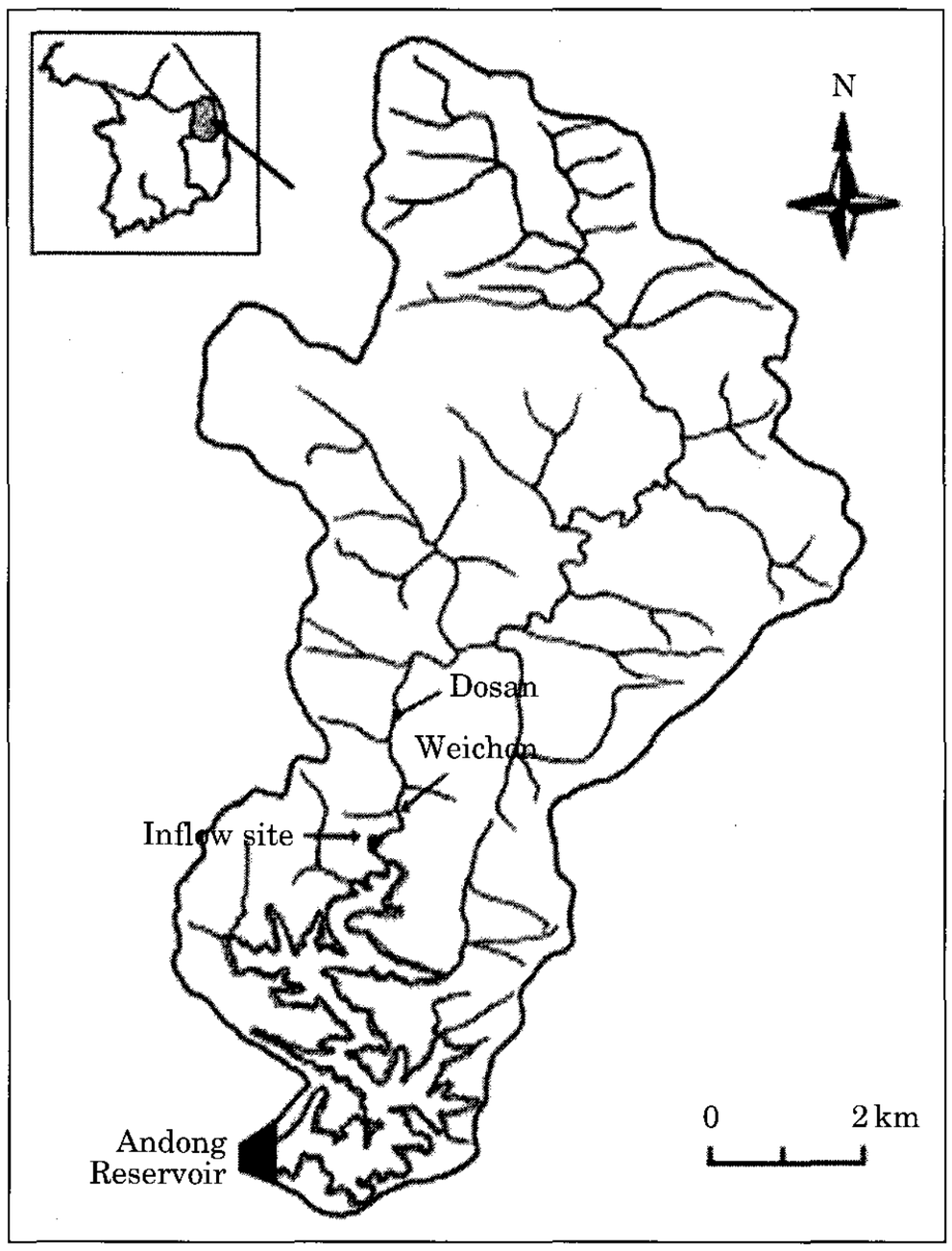

Fig. 1. Map of watershed of Andong Reservoir.

The hydro-morphological characteristics of Andong Reservoir are presented in Table 1.

The Andong Reservoir area is characterized by hot, humid summers and cool, dry winters. The coldest monthly mean temperature generally occurs in January (3.9°C), while the warmest month is usually August (25.4°C). The prevailing winds are southeasterly in summer, and northwesterly in winter. The winds are stronger in winter, from December to February, than those of any other season. The rainy season over Korea, the so-called Jangma season, continues for a month from late June until late July. A short period of rainfall comes in early September when the monsoon front retreats back from the north. This seasonal march of the Asian summer monsoon season accounts for almost 75% of the total yearly average precipitation. Usually, the torrential rainfalls are concentrated in an episode of just a few days and the overflow has lower temperature (Fig. 2). Such inflows have large density, not only because of lower temperature, but also due to very high concentration of suspended and dissolved solids (Jiahua, 1986; Alavian *et al.*, 1992).

Table 1. Hydro-morphological characteristics of Andong Reservoir (KWATER, 2005).

Catchment	Area (km^2)	1,584
	Annual average inflow ($m^3\ sec^{-1}$)	32.6
	Annual average precipitation (mm)	1,148.4
Reservoir dimension and structure	Water capacity ($\times 10^6\ m^3$)	1248
	Average water volume ($\times 10^6\ m^3$)	587
	Surface area (km^2)	51.5
	Ratio of watershed to lake surface area	3 : 1
	Maximum depth (m)	60
	Maximum length of main axis (km)	43.5
	Mean width (km)	1.2
	Maximum surface water elevation (m)	161.7
	Average surface water elevation (m)	143.8
	Elevation of outlet for intake tower (m)	121 ~ 129
	Elevation of lake bottom (m)	92

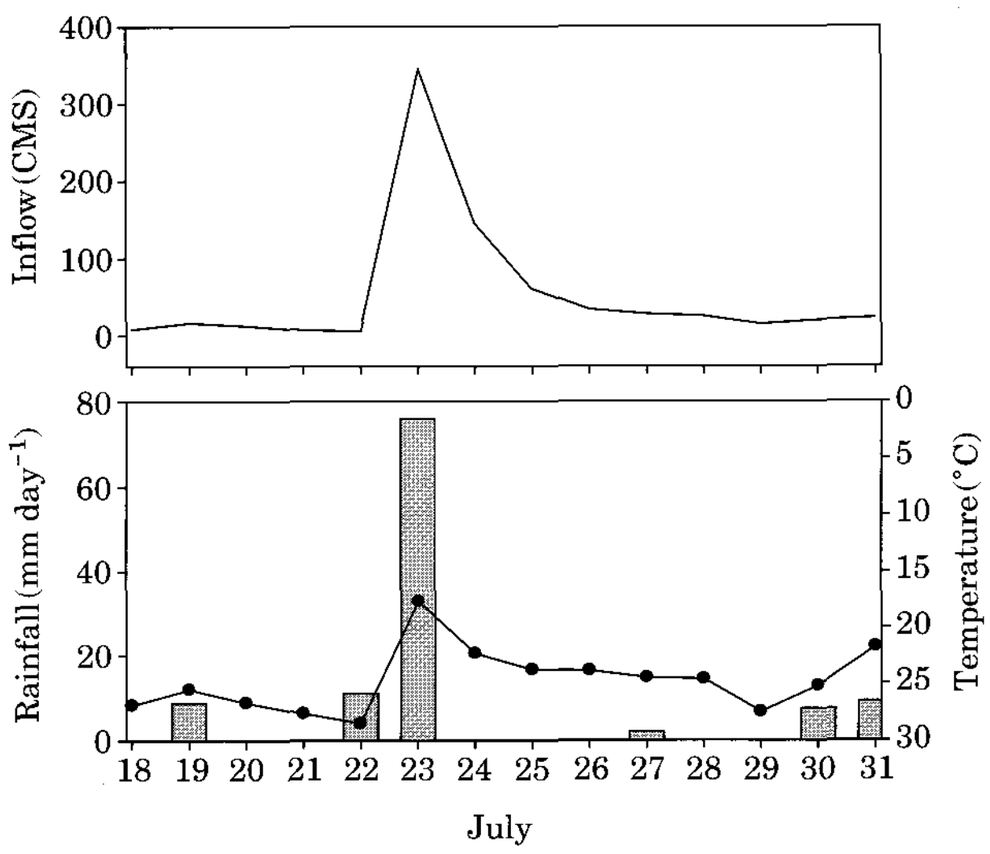

Fig. 2. Daily variations of the inflow rate and the water temperature of the main inflow and the rainfall during the summer monsoon season.

Such inflows generally enter the reservoir as a turbid density current. As it moves along the stratified reservoir, it takes the form of interflow because the density of inflow is greater than that of the epilimnion while lesser than that of the hypolimnion. Andong Reservoir beings to stratify

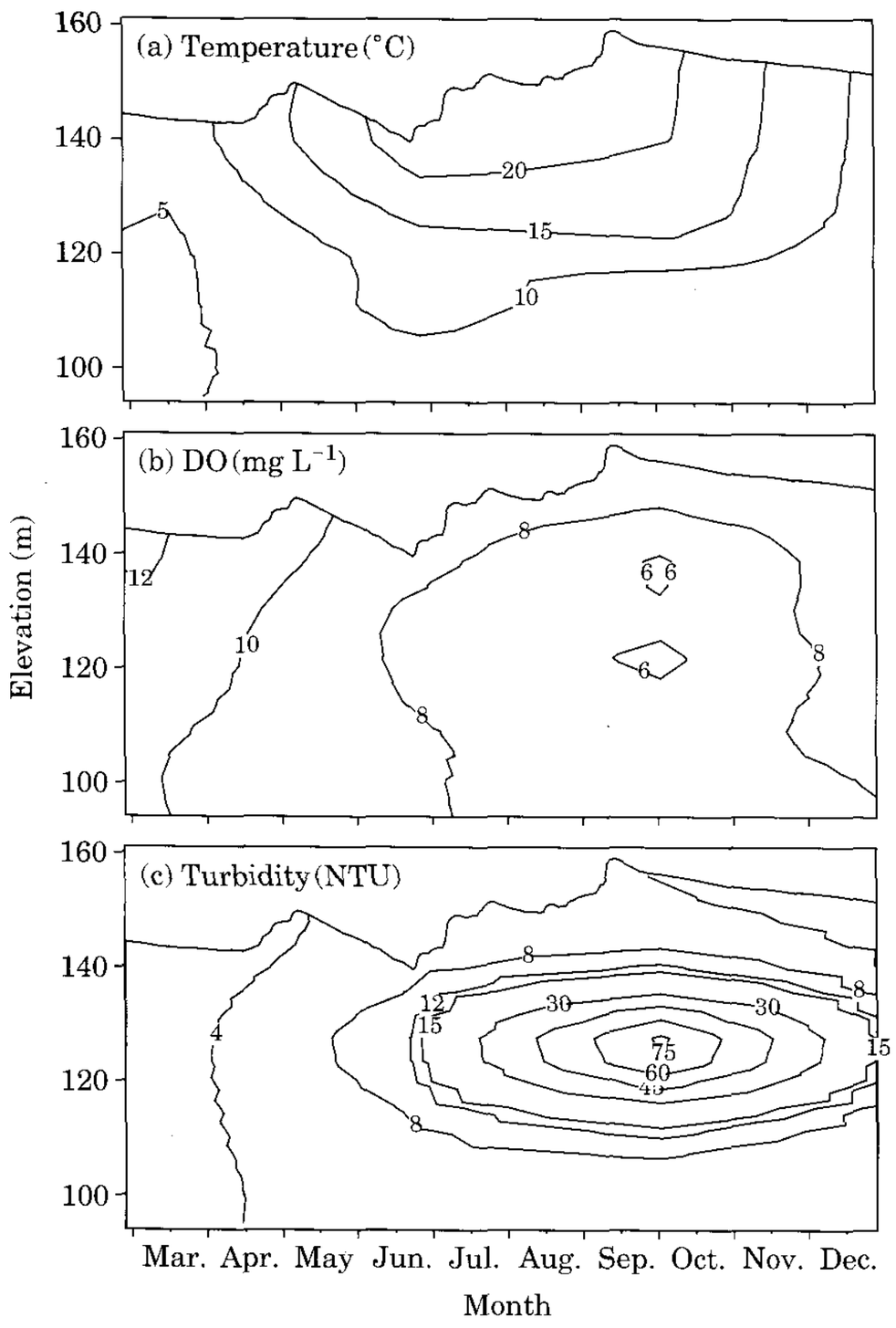

Fig. 3. Distribution of (a) temperature, (b) dissolved oxygen, and (c) turbidity in Andong Reservoir for the year 2003.

from summer onwards and turnover occurs in winter. The interflowing density currents, usually form a thickness of 10~15 m, and move along the metalimnion of the Andong Reservoir; until being finally discharged through the outlet. Such interflows, with high concentrations of organic matter and nutrients, usually results in an oxygen deficiency and phytoplankton bloom (Wunderlich, 1971; Soltero *et al.*, 1974). The dissolved oxygen profile shows hetrogrades (positive and negative), which are common occurrences in stratified water (Wetzel, 1983). The occurrence of metalimnetic minimum, also known as negative heterograde curve, is a common dissolved oxygen distribution pattern in deep reservoirs of temperate region (Walker, 1987; Cole and Hannan, 1990). The typical yearly distribution of temperature, dissolved oxygen and turbidity is shown in Fig. 3.

As, the CE-QUAL-W2 model, a two dimensional, longitudinal/vertical, hydrodynamic, and water quality model, is based on the finite difference solution of laterally averaged governing equations for momentum and constituent transport, it is best suited for relatively long and narrow waterbodies exhibiting longitudinal and vertical water quality gradients (Cole and Wells, 2003), such as the reservoir being studied.

The Nakdong River system is dotted with numerous reservoirs and Andong Reservoir, being strategically situated in the uppermost chain of reservoirs, also has a greater role as a control point for series of reservoirs located in its immediate downstream. Therefore, a deeper understanding of the characteristics of Andong Reservoir is crucial to address the direct and indirect management issues of, not only Andong Reservoir itself but also of the series of other reservoirs located in its downstream. Thus, the purpose of this study was to apply the CE-QUAL-W2 model in Andong Reservoir to simulate its distinctive hydro-thermal and its influence on the dissolved oxygen regimes and transport of density current.

MATERIALS AND METHODS

1. Model description

A two dimensional (2-D), laterally averaged hydrodynamic and water quality model, CE-QUAL-W2, was developed by Environmental and Hydraulics Laboratories of the US Army Engineer Waterways Experiment Station (WES) as a tool for water resource management.

The CE-QUAL-W2 model's advection-diffusion equations describing laterally averaged fluid motion and mass transport are solved by using the finite-difference method. The model's equations that describe horizontal momentum, free water surface elevation, hydrostatic pressure, continuity, equation of state, and constituent transport, have been presented previously (Chung and Gu, 1998; Cole and Wells, 2003). The model assumes that vertical velocities are sufficiently small to allow the vertical momentum equations to be simplified in the hydrostatic equation. All the governing equations used in the model are based in a 2D Cartesian coordinate system (Cole and Buchak, 1995).

A stable stratification hampers the vertical mo-

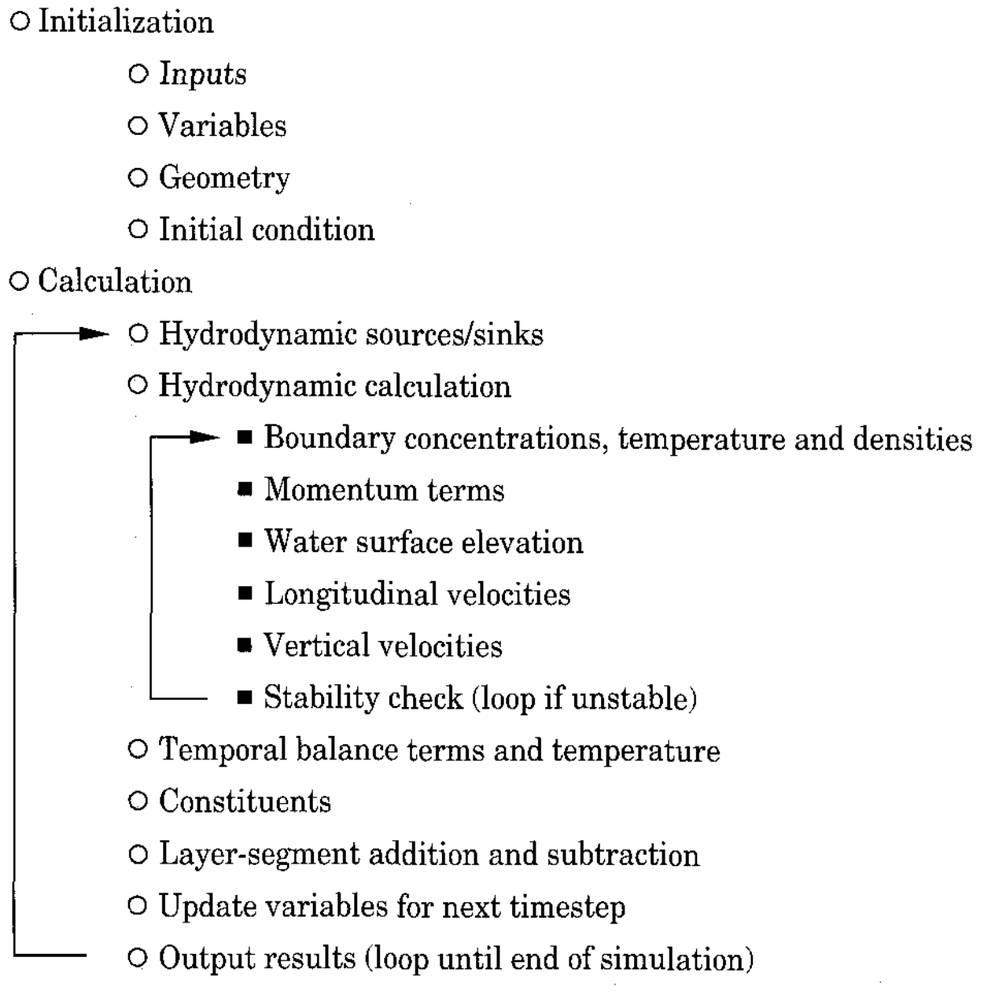

Fig. 4. Solution structure of CE-QUAL-W2 model.

vement of water and constituents. The effect of stratification on turbulent transport is taken into account by correction to vertical turbulent dispersion coefficient (D_z) under nonstratified conditions with a local Richardson number defined by velocity and density gradients (Orlob, 1983; Cole and Buchak, 1995). D_z is calculated from velocity gradient, depth, water density distribution or reservoir stratification, bottom shear, and surface wind shear (Buchak and Edinger, 1982; Cole and Buchak, 1995). A default value ($1\ m^2\ s^{-1}$) for the longitudinal dispersion coefficients (A_x for momentum and D_x for mass) is used in this study. This default value is based on model testing against field data for numerous reservoirs under a wide variety of conditions (Cole and Buchak, 1995).

CE-QUAL-W2 updates hydrodynamics, inflow and outflow at each computational time-step. Hydrostatic stability is maintained through autostepping; an algorithm embedded in the model that calculates the maximum allowable timestep locally at each node. The average time step was 360 seconds over the simulation period. The schematic of the CE-QUAL-W2 model solution structure is shown in Fig. 4.

The heat budget of the model includes terms for evaporative heat loss, short- and long-wave radiation, convection, conduction and back radiation (Cole and Wells, 2003). Surface heat exchange is calculated as a term-by-term process. Incident short wave radiation, wind speed, air temperature, dew point temperature, cloud cover and water surface temperature are used to calculate the net rate of heat exchange across the water surface. The computation is explicit, whereby water surface temperatures are used from the previous time step.

Major chemical and biological processes in CE-QUAL-W2 include the effects on DO of atmospheric exchange, photosynthesis, respiration, organic matter decomposition, nitrification, and chemical oxidation of reduced substances; uptake, excretion, and regeneration of phosphorus and nitrogen and nitrification-denitrification under aerobic and anaerobic conditions; carbon cycling and alkalinity-pH-CO_2 interactions; trophic relationships for total phytoplankton; accumulation and decomposition of detritus and organic sediment; and coliform bacteria mortality. All decay and decomposition processes in the model flow first order kinetics. More than sixty chemical and biological rate coefficients and other parameters are required for the application of CE-QUAL-W2 (Table 3). Most of the parameter values were based on suggestions given in the CE-QUAL-W2 manual (Cole and Buchak, 1995), and all the parameters are temporally and spatially constant. Some of the parameters have suggested ranges, and selected parameters were adjusted, within reasonable limits, until simulated values agreed with measured observations (calibration).

The settling velocity of each inorganic suspended solids [ISS] compartment is a user-defined parameter. Usually, this is determined from Stoke's settling velocity for a particular sediment diameter and specific gravity. For further details on the remaining constituents, the reader is referred to Cole & Buchak (1995).

2. Bathymetry data and the model grid

The Andong Reservoir CE-QUAL-W2 model bathymetry was based on the sediment survey and design specification for Andong Reservoir (KWATER, 1996). Without the boundary segments and layers, the final model grid had a single main branch and consisted of 22 segments, and 69 layers. Each model cell had an assigned cell width. Segments ranged from 2 km in length to less than 500 meters. A height of 1.0 meter

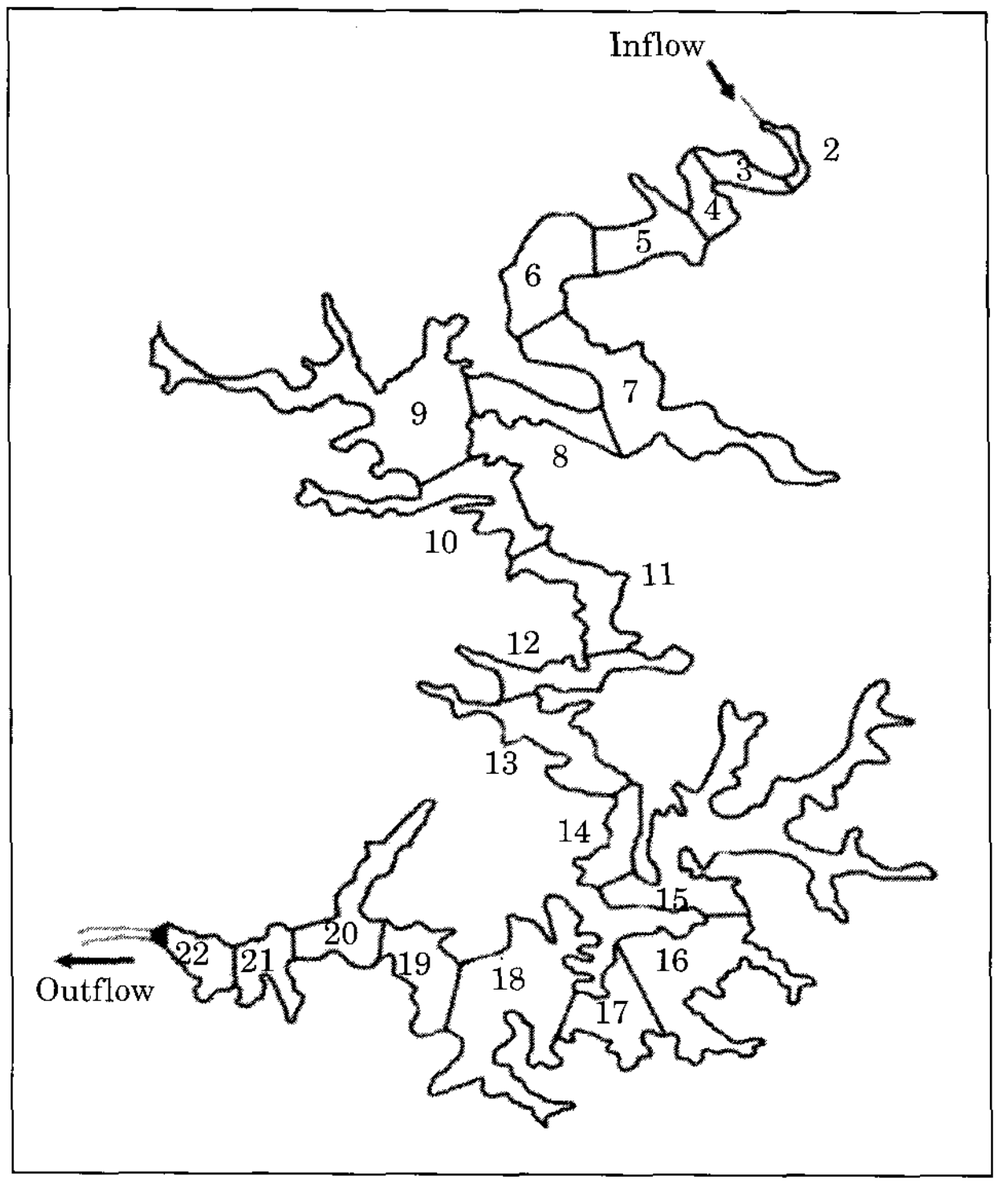

Fig. 5. Segments of Andong Reservoir model superimposed on the Andong Reservoir.

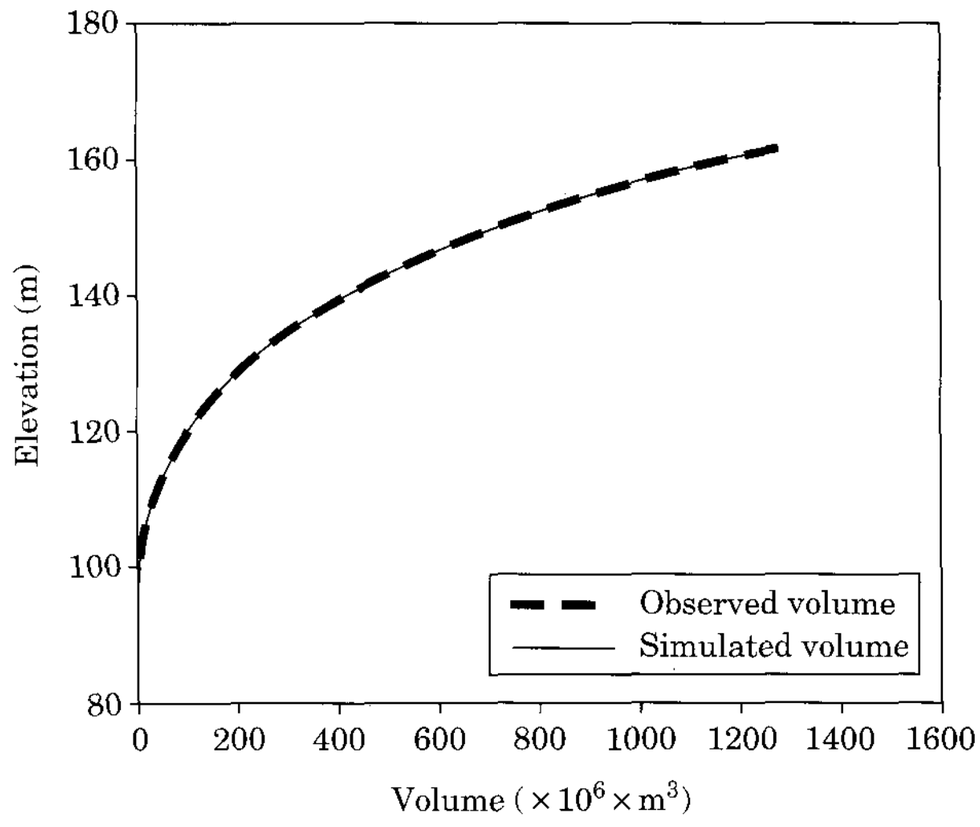

Fig. 6. Observed and simulated water volume-elevation curves for Andong Reservoir.

was specified for all the layers. The model domain covers a total distance of about 44.7 km from the dam site up to the riverine zone. The bathymetrical model grid superimposed on the Andong Reservoir is shown in Fig. 5.

The accuracy of bathymetry data was checked using storage-capacity curve which shows the reservoir storage at different reservoir elevations (Fig. 6). The bathymetry generated for the model has a 0.3% error from the sediment survey storage-capacity curve for the year 1996.

3. Meteorological data

Most of the meteorological data used in this study were obtained from the Andong station of Korean Meteorological Association (KMA, 2004). The meteorological data-sets used were: air temperature, dew point temperature; wind speed, wind direction, and cloud cover observations. The measurement data were collected on the hourly basis but their daily mean values were used in the model. Air temperature was used as a surrogate for precipitation temperature.

4. Hydrological data

The daily data of stream flow and water temperature generated at Dosan station and the daily record of precipitation from Weichon station were used in the model (Fig. 1). The rest of the data used this hydrodynamic model originated at the deepest section of the Reservoir (the main dam site). Temperature, dissolved oxygen and turbidity, for depths of 0 through 45 m, were directly measured using a multi-parameter probe (YSI, 6000) at various frequencies throughout the simulation period. The water samples were collected using PVC Van Dorn sampler from the various depths in the dam site as well as from the inflow stream. The samples were filtered using Whatman GF/C filter papers in the lab. The filter papers were dried to a constant weight at 103 to 105°C, and their residue weight was used to calculate the total suspended solids concentration.

Andong reservoir has two identified outflow pathways: outflow through the powerhouse intake and outflow over the spillway. The intake tower, a single withdrawal structure, draws water for the power plant using only one intake elevations (121 m to 129 m) and is predominantly operated throughout the year to send the water though a powerhouse and then to the downstream. The spillway has a total design discharge capacity of 5,200 m^3 sec^{-1} and is controlled by 4 radial gates, which are 14.0 m by 9.5 m (width by

height, respectively) each and is primarily used for the only purpose of flood control. The daily data of discharges from the designated outlets as well as of surface water elevation were provided by KWATER (KWATER, 2005).

5. Assumptions

Due to the lack of quantitative data to describe many aspects of the Andong Reservoir system, a number of following key assumptions were made during development of the hydrodynamic model:

- The branches and tributaries of Andong Reservoir were not characterized in the model, due to the lack of their flow information and their depth-volume profile data. It is assumed that, they don't have a significant influence on the water quantity balance, due to the negligible flows associated with them.
- The reservoir bottom is assumed to be an immobile and impermeable boundary i.e. the bottom sediments are stationary and not re-suspended by flow and ground-water discharge to the reservoir or recharge from the reservoir to ground water is negligible.
- The reservoir bottom extracts energy from water movement by causing resistance to water flow; this phenomenon varies with the magnitude of flow. A single, empirical coefficient (Chezy resistance coefficient) is applied to the reservoir bottom in all the computational segments.
- The heat exchange from the reservoir bottom is about two orders of magnitude less than surface heat exchange (Cole and Buchak, 1995). We assumed this to hold true in estimation of sediment temperature from the annual average water temperature near the sediment-water interface. Also, the sediment temperature and the exchange coefficient are assumed to be temporally and spatially constant for all the segments.
- Topographic shading effects on water temperature are insignificant.

6. Evaluation of model performance

The model performance can be evaluated by the "Root Mean Square Error" (RMSE) statistic (e.g. Thomann 1982). The RMSE is proposed as a general test that can be used to evaluate the correspondence, or goodness of fit, between predicted values from mathematical models and observed data. Thus, the test allows inference of a model's capability. The RMSE is computed from:

$$RMSE = \sqrt{\frac{\Sigma(predicted - Observed)^2}{Numberofobservations}}$$

The RMSE becomes larger as measured and observed values diverge, with a RMSE of 0 indicating a perfect prediction.

RESULTS AND DISCUSSION

This hydrodynamic module of CE-QUAL-W2 model for Andong Reservoir was calibrated for the year 2003, and verified though a single continuous run from January, 2000 till December, 2004.

1. Water levels

The first step in the hydro-dynamic calibration of CE-QUAL-W2 model for Andong Reservoir was carried out by ensuring that the model correctly predicted water levels at the dam site.

At mid-summer, the Andong Reservoir surface water is at the lowest and such draw-downs are timed to coincide as nearly as possible with the beginning of monsoon season. The highly intense runoffs generated in short period leads to vast erratic surface water level variation that greatly effects the bio-chemico-physical composition of the water body (e.g. Gloss *et al.*, 1980; Dirnberger *et al.*, 1986; Lind *et al.*, 1992; Laenen and LeTourneau, 1996; Gibson *et al.*, 1997). The short term surface water level fluctuations in Andong Reservoir are of greater magnitude than the monthly averages. For e.g., in August 7th, 2002, when the typhoon Rusa passed by, a record of 3499.293 CMS of inflow was generated and just in that single day, the reservoir water level rose by 8.8 m from 145.93 m to 154.75 m.

The initial water surface was set at the maximum of 143.36 meters and the default bottom roughness of 70 suggested in the CE-QUAL-W2 manual was assigned for each segment. The water balance was achieved without any major changes to the default value provided in the model's manual. Time series of the observed and modeled water levels of Andong Reservoir for the calibration year of 2003 is shown in Fig. 7. The predicted elevations were almost an exact overlay of the observed values. Root mean square error (RMSE)

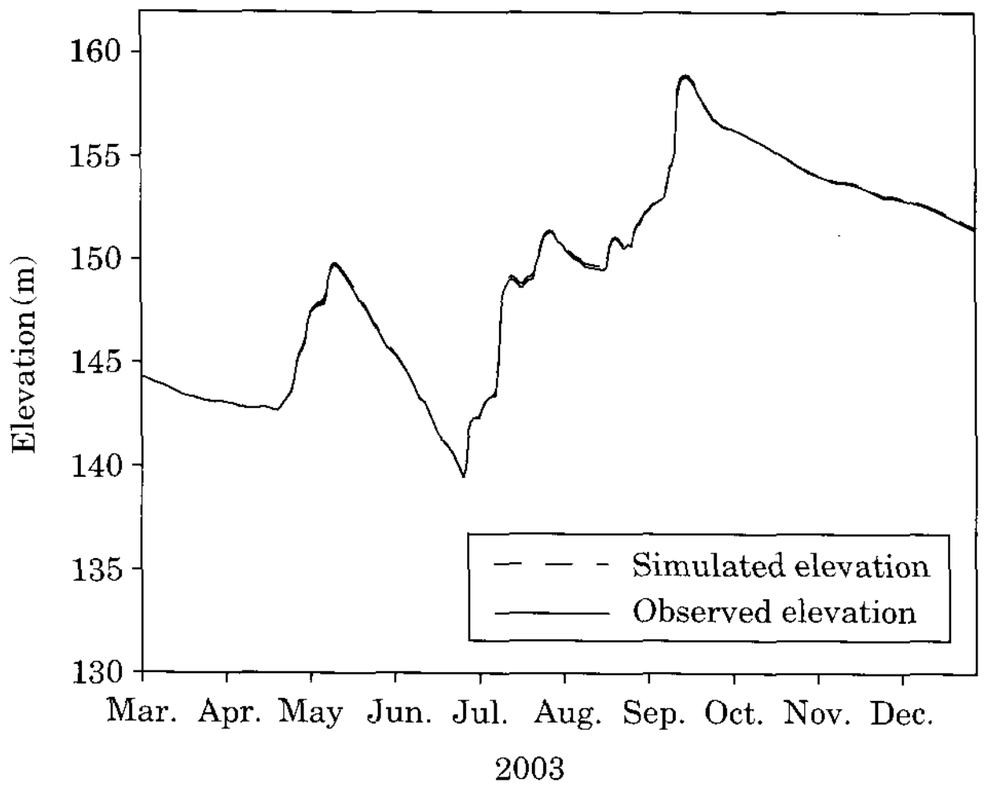

Fig. 7. Observed and simulated surface water elevation for Andong Reservoir.

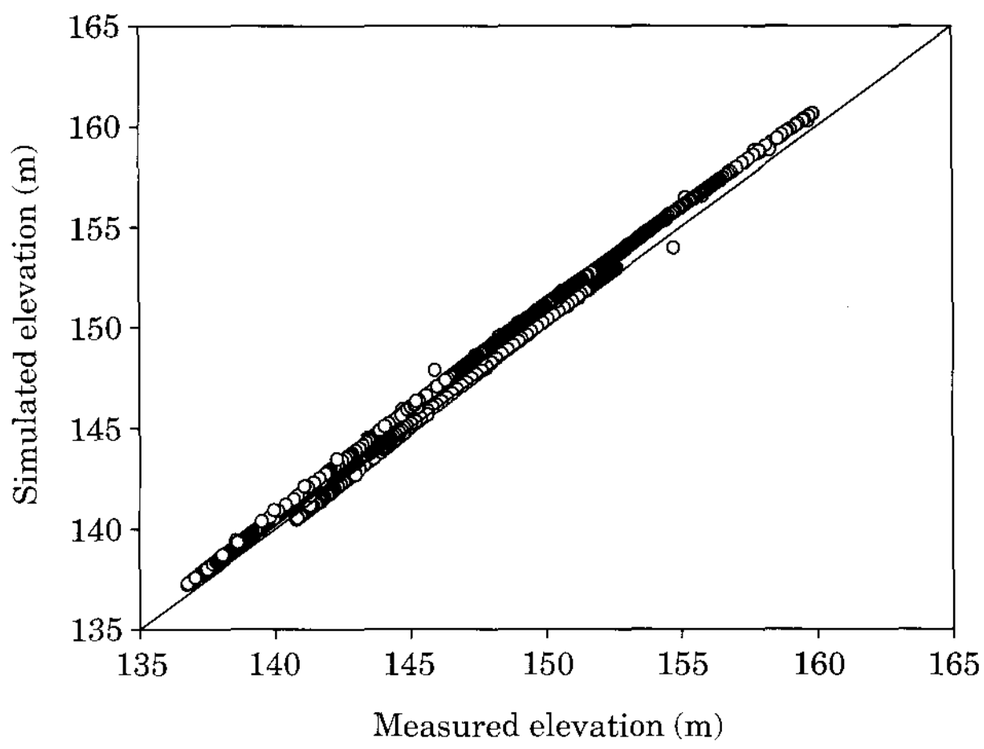

Fig. 8. Result of verification of water surface elevation from 2000~2004. Diagonal line is the line of slope 1 (i.e. observed=simulated).

of model water level predictions during the calibration was 0.095 m. Having a precise and accurate bathymetry was crucial factor in modeling surface water level of Andong Reservoir.

Reservoirs modeled using CE-QUAL-W2 generally uses upstream inflows and downstream outflows, therefore, it is important that these flows balance; otherwise the reservoir water surface elevations may rise or fall unrealistically. So, although the simulation period had events of intense short-term fluctuations in water-level, the model simulated surface-water level with high accuracy. The statistical comparison of the simulated and observed water level elevations showed the root mean square error (RMSE) of 0.763 m. The water balance achieved for Andong Reservoir during the verification run is shown in Fig. 8.

2. Temperature and thermal stratification

For the Andong Reservoir Model, hydrodynamics and thermodynamics were calibrated together as they are strongly coupled. Thermal stratification influences internal currents while advection modifies the temperature field. The thermal structure was considered to be calibrated when the temperature field met the quantitative criteria. Default hydraulic parameters were used to run the model initially. With each model run, these parameters were adjusted to achieve a unique set of coefficients that best represented the system under all conditions. In general, the thermal balance of Andong Reservoir was highly an inflow driven event. Simulations runs showed that the wind doesn't had noticeable affect on stratification of Andong Reservoir, which might be due to the strong stability generated by its great depth. The wind-sheltering coefficient [WSC] was set to a constant value since there is no visible vegetation throughout the majority of the watershed that could potentially modify the wind velocity. Table 2 shows the parameters and their values calibrated used in the thermal calibration.

The temperature calibration involved comparing vertical temperature profile data with model predicted temperatures from a single location (dam site) for the year of 2003. Simulated profiles were output daily and compared to field data (Fig. 9), and statistics were calculated on differences between the model and data. The model also performed well in simulating descending thermocline, simulating timing of turnover, onset of stratification, and duration of stratification (Fig. 9). From December through March, Andong Reservoir was typically isothermal and cold. Surface temperatures began to warm in April due to increased solar radiation, and continued to do so throughout May. By May, thermocline developed at depths between 5 and 15 m and subsequently the stratification begins and persisted until October~November. This distinct vertical temperature gradient develops in the summer due to the absorption of solar and

Table 2. Model parameters affecting temperature calibrations.

Parameters	Variable	Unit	Default	Calibrated
Horizontal Eddy viscosity	AX	$m^2 s^{-1}$	1.0	1.0
Horizontal eddy diffusivity	DX	$m^2 s^{-1}$	1.0	1.0
Chezy bottom friction factor	CHEZY	$m^{1/2} s^{-1}$	70	70
Wind-sheltering	WSC	–	0.85	0.5
Solar radiation fraction absorbed at surface	BETA	–	0.45	0.6
Solar radiation extinction-detritus	EXOM	m^{-1}	0.1	0.04
Solar radiation extinction-algae	EXA	m^{-1}	0.2	0.2
Solar radiation extinction-water	EXH_2O	m^{-1}	0.25	0.45
Sediment temperature	TSED	°C	–	10
Coefficient of bottom heat exchange	CBHE	$Wm^2 s^{-1}$	0.3	0.5

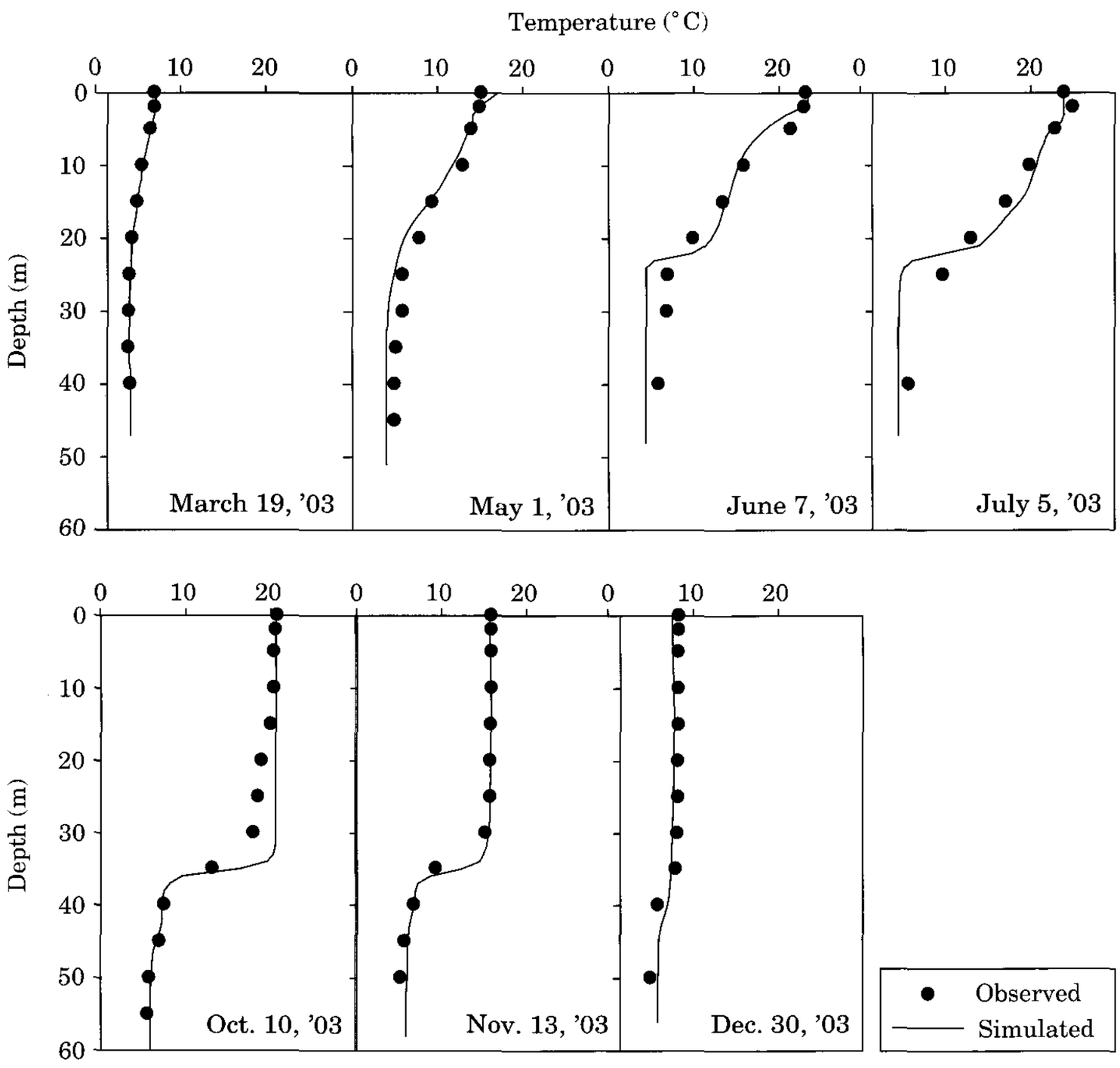

Fig. 9. Calibration results of vertical temperature profiles at different seasons.

atmospheric radiation in the upper part of the lake's water column. The density difference between the warmer surface water in the epilimnion and the denser colder water in the hypolimnion isolated the water below the reservoir outlet in summer. Later in the year, as solar radiation and air temperature decreased, the temperature of the lake surface cooled from late-October onwards, and eventually, by late-December the densities of the surface and deep water were similar enough to allow the lake to "turn over" and become isothermal again. The effect of storm water inflow of 1887.1 CMS in mid-September was still seen at the temperature profile of early October at the layers between depths of 15~30 m, where the thermocline is a bit sharper

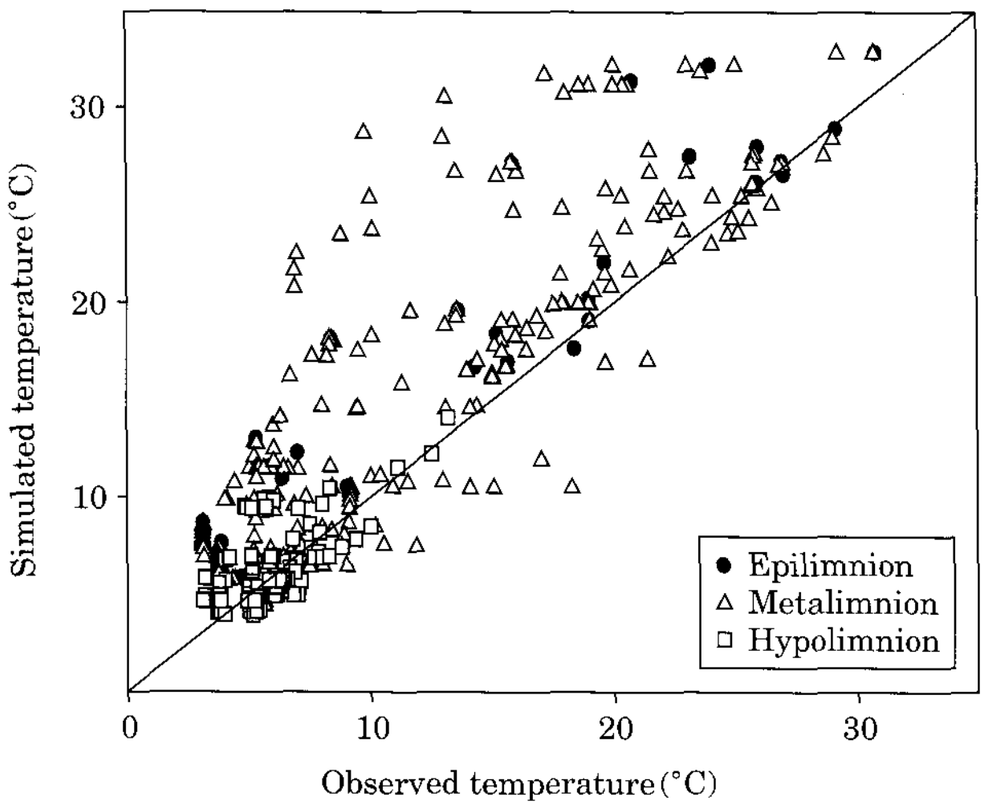

Fig. 10. Result of verification of temperature from 2000~2004. Diagonal line is the line of slope 1 (i.e. observed=simulated).

for predicted values, as it generated additional mixing in the entrainment layer between hypolimnion and epilimnion. The RMSE value for temperature calculated from observations at dam site for all days of sampling for 2003 was 1.82°C.

The verification of temperature was done through a single continuous run from 2000~2004. The results were compared with the fluctuations of temperature at epilimnion (depth 0 m), metalimnion (depth 30 m), and hypolimnion (>30 m) (Fig. 10). The RMSE values calculated for all the measured data for temperature was 4.91°C. The hypolimentic temperature for the year of 2002 is over-predicted during the verification run. This is likely a result of improperly modeled internal waves during the storm discharge of 3499.29 CMS inflow in a single day by typhoon Rusa on early August, 2002.

Clearly, interpretation of model output must be tempered with the realization that:

- Temperature and other water quality predictions can exhibit a fairly large change from one day to the next.
- Temperature predictions are averaged over the length, height and width of a cell. Observed data represents observations at a specific point within the reservoirs, and
- Computed temperatures are subject to large daily variations depending upon how rapidly inflows, outflows, and meteorological inputs are changing (Cole *et al.*, 1997).

3. Dissolved oxygen dynamics

Dissolved Oxygen has particular importance in lake and reservoirs. As stated by Hutchinson "[one] can probably learn more about the nature of a lake from a series of oxygen determinations than from any other kind of chemical data" (Hutchinson, 1957). Besides improving understanding of the system, modeling DO is another method of improving hydrodynamic accuracy of the existing model. According to the CE-QUAL-W2 user's manual "experience has shown that DO and phytoplankton are often much better indicators of proper hydrodynamic calibration than either temperature or salinity" (Cole and Wells, 2003).

DO is a more complex parameter than either temperature or salinity. There are many mechanisms which affect oxygen's solubility, replenishment, and consumption which the model development simulates. Factors that affect the concentration of dissolved oxygen in reservoirs include water temperature, inflows and outflows, algal photosynthesis and respiration, zooplankton respiration, ammonia nitrification, decomposition of organic matter in the sediments and water column, and exchanged with the atmosphere (Cole and Hannan, 1990).

The vertical profiles of DO from monitoring data in Andong Reservoir show seasonal and spatial distribution variations. Fig. 11 shows that the calibration results of DO minimum phenomenon matched well with the measured profiles. Cold water has higher capacity to hold dissolved oxygen as seen from December through March. As the surface of the reservoir starts to warm, oxygen solubility decreased and surface concentrations decreased via losses to the atmosphere. The bacterial decomposition of dead algae and other organic matter in lake sediments can consume substantial amounts of oxygen, which is taken from the overlying water column. Later, the stratification of the lake isolates the hypolimnion and its oxygen gradually depletes, primarily due to the sediment oxygen demand.

On 5th July, 2003, a metalimnetic oxygen minimum occurs just beneath the thermocline at a depth of 10 m with oxygen concentration of <5 mg L^{-1}, the oxygen concentration then gradually increases up to the deeper layers. This phenome-

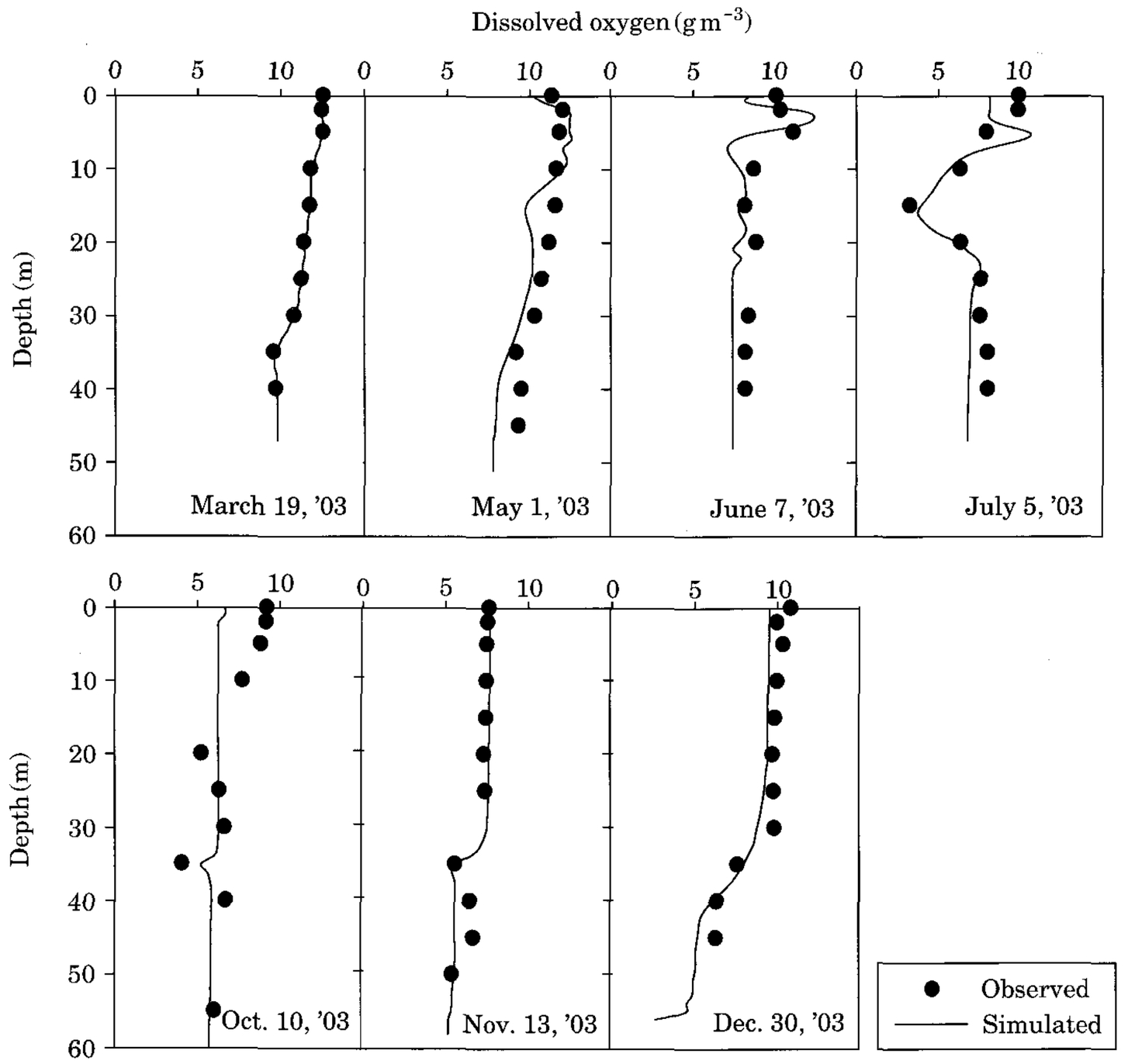

Fig. 11. Calibration results of vertical DO profiles in different seasons.

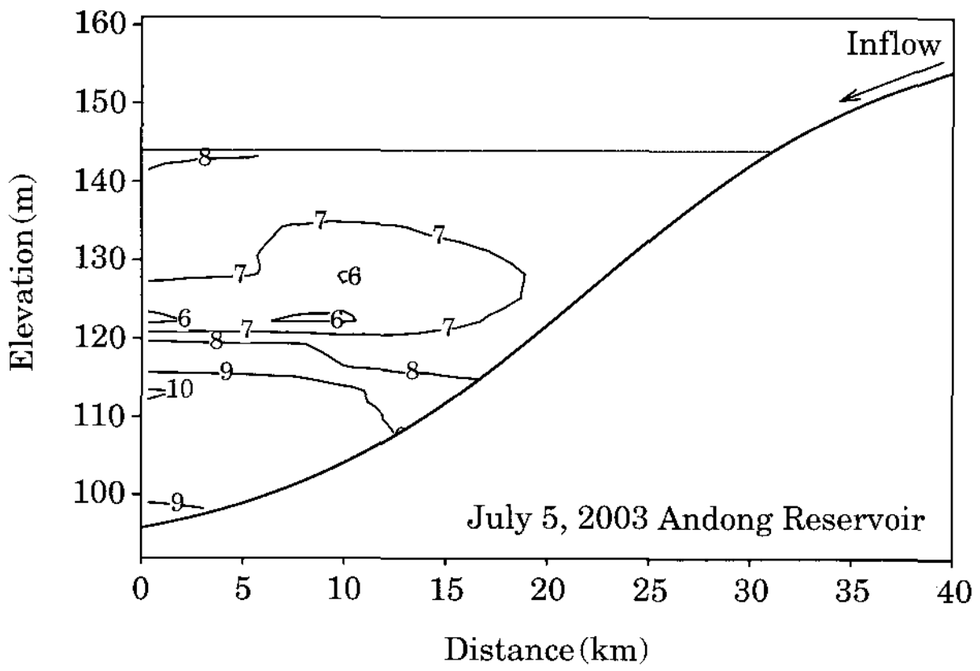

Fig. 12. The depth-distance profile of dissolved oxygen in Andong Reservoir.

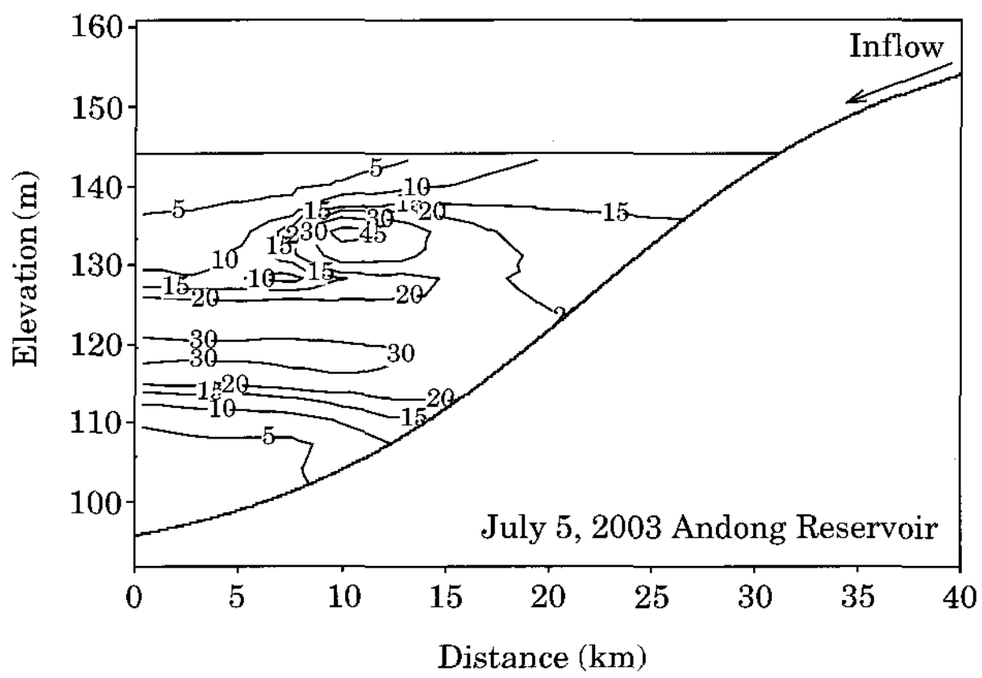

Fig. 13. The depth-distance profile of Turbidity (NTU) in Andong Reservoir.

non of metalimnetic oxygen minima has been frequently observed in Andong Reservoir around June and July which coincides with the algal growth period and also in late summer after heavy rainfall season (Heo *et al.*, 1998; An *et al.*, 2000; Park *et al.*, 2006).

The layer of reduced dissolved oxygen concentration on 5th July, 2003 stretches laterally and could be identified through the whole lake from the dam to the upstream section (Fig. 12).

Table 3. Model parameters used for calibration of dissolved oxygen dynamics.

Parameters	Variable	Unit	Default	Calibrated
Algae				
Growth rate	AG	day^{-1}	2.0	1.8
Mortality rate	AM	day^{-1}	0.1	0.05
Excretion rate	AE	day^{-1}	0.04	0.02
Respiration rate	AR	day^{-1}	0.04	0.12
Settling rate	AS	$mday^{-1}$	0.1	0.01
Phosphorus half-saturation for algal growth	AHSP	$gday^{-3}$	0.003	0.005
Nitrogen half-saturation for algal growth	AHSN	$gday^{-3}$	0.014	0.30
Light saturation intensity	ASAT	Wm^{-2}	75	55
Fraction of algae to POM	APOM	–	0.8	0.8
Lower temperature for minimum algal rates	AT1	°C	5	6
Upper temperature for minimum algal rates	AT2	°C	25	16
Lower temperature for maximum algal rates	AT3	°C	35	25
Upper temperature for maximum algal rates	AT4	°C	40	30
Lower temperature rate multiplier for minimum algal rates	AK1	–	0.1	0.1
Upper temperature rate multiplier for minimum algal rates	AK2	–	0.99	0.99
Lower temperature rate multiplier for maximum algal rates	AK3	–	0.99	0.99
Upper temperature rate multiplier for maximum algal rates	AK4	–	0.1	0.1
Phosphorus to biomass ratio	BIOP	–	0.005	0.001
Nitrogen to biomass ratio	BION	–	0.08	0.08
Carbon to biomass ratio	BIOC	–	0.45	0.45
Algae to chlorophyll *a* ratio	ACHLA	–	45.0	67
Phosphorus				
Sediment release rate of phosphorus	PO4R	day^{-1}	0.001	0.001
Fraction of phosphorus in Organic Matter	ORGP	day^{-1}	0.005	0.001
Ammonium				
Ammonium decay rate	NH4DK	day^{-1}	0.12	0.08
Sediment release rate of ammonium (fraction of SOD)	NH4R	–	0.001	0.01
Lower temperature for ammonium decay	NH4T1	°C	5	4
Upper temperature for ammonia decay	NH4T1	°C	25	25
Lower temperature rate multiplier for ammonium decay	NH4K1	–	0.1	0.1
Upper temperature rate multiplier for ammonium decay	NH4K2	–	0.99	0.99
Nitrate				
Nitrate decay rate	NO3DK	day^{-1}	0.03	0.05
Lower temperature for nitrate decay	NO3T1	°C	5	5
Upper temperature for nitrate decay	NO3T2	°C	25	25
Lower temperature rate multiplier for nitrate decay	NO3K1	–	0.1	0.1
Upper temperature rate multiplier for nitrate decay	NO3K2	–	0.99	0.99
Carbon				
Labile DOM decay rate	LDOMDK	day^{-1}	0.10	0.1
Refractory decay rate	RDOMDK	day^{-1}	0.001	0.001
Labile to refractory DOM Decay rate	LRDDK	day^{-1}	0.01	0.01
Labile POM decay rate	LPOMDK	day^{-1}	0.08	0.08
Labile to refractory POM Decay rate	LRPDK	day^{-1}	0.01	0.001
POM settling rate	POMS	ms^{-1}	0.1	0.01
Fraction of algae to POM	APOM	–	0.8	0.8
Fraction of carbon in organic matter	ORGC	–	0.45	0.45
Lower temperature for OM decay	OMT1	°C	5	4
Upper temperature for OM decay	OMT2	°C	25	30
Lower temperature rate multiplier for OM decay	OMK1	–	0.1	0.1
Upper temperature rate multiplier for OM decay	OMK2	–	0.99	0.99

Table 3. Continued.

Parameters	Variable	Unit	Default	Calibrated
Oxygen				
Oxygen limit for anaerobic processes	O2LIM	$g\,m^{-3}$	0.1	0.1
Stoichiometric ratio for nitrification	O2NH4	–	4.57	4.57
Oxygen stoichiometric ratio for organic matter decay	O2OM	–	1.4	1.4
Stoichiometric ratio for algal respiration	O2AR	–	1.1	1.1
Stoichiometric ratio for algal growth	O2AG	–	1.4	1.4
Sediment				
Sediment decay rate	SEDK	day^{-1}	0.1	0.01
Zero-order sediment oxygen demand	SOD	$gm^{-2}day^{-1}$	0.1~1.0	0.2
Lower temperature for sediment decay	SODT1	°C	4	4
Upper temperature for sediment decay	SODT2	°C	25	25
Lower temperature rate multiplier for sediment decay	SODK1	–	0.1	0.1
Upper temperature rate multiplier for sediment decay	SODK2	–	0.99	0.99

The depth-distance profile of Turbidity (NTU) in Andong Reservoir during the same period also shows high concentration of suspended solids (Fig. 13). Also, the vertical profile of chlorophyll *a* shows higher concentrations during the same period (figure not included). Thus, dissolved oxygen minima formation in the metalimnion layer of Andong Reservoir is the result of different complex processes. The upper part of DO minima layers formation on the interface of epilimnion and metalimnion is related to organic activity in the surface, and the lower part of those was the result of turbid water inflow to metalimnion during rainy season (Park *et al.*, 2006).

The RMSE value for dissolved oxygen calculated from observations at dam site for all days of sampling for 2003 was 1.13 mg L^{-1}. Boundary conditions, algae growth, photosynthesis & respiration rates, reaeration equation and sediment oxygen demand were particularly important for model calibration. Some of the more relevant model parameters used for the calibration of dissolved oxygen dynamics are presented in Table 3.

The verification of dissolved oxygen concentration was done through a single continuous run from 2000~2004. The results were compared with the distribution of dissolved oxygen concentration at epilimnion (depth 0 m), metalimnion (depth 30 m), and hypolimnion (>30 m). The RMSE values calculated for all the measured data for dissolved oxygen concentration was 1.37 mg L^{-1} (Fig. 14).

The typical seasonal patterns of temperature and dissolved oxygen that occur in the Andong Reservoir are illustrated by the modeled longitudinal slices on selected dates in 2003 (Fig. 15).

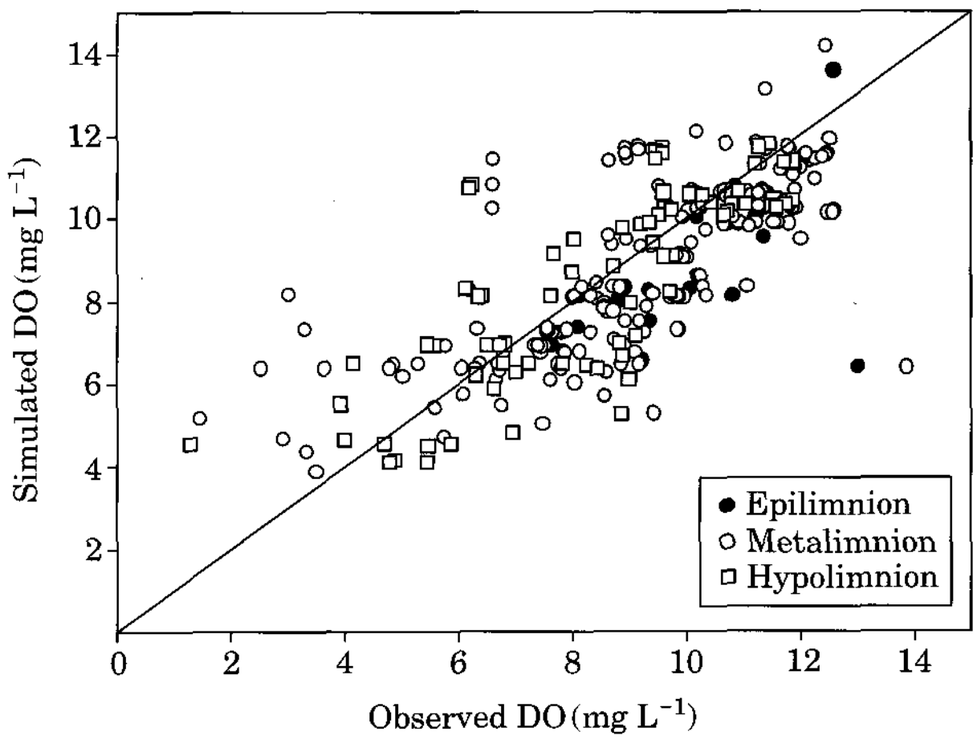

Fig. 14. Result of verification of DO from 2000~2004. Diagonal line is the line of slope 1 (i.e. observed= simulated).

4. Modeling transport of density flow

The settling velocity of particulate matters in water depends upon the particle's diameter and density. Apparently, many of the larger particles mobilized in the stream during the high runoff interval are deposited before reaching lacustrine portions of the reservoir. This size sorting process operates widely in reservoirs, manifested as higher sediment deposition (Effler *et al.*, 2001; Effler and Matthews, 2004) and accumulation

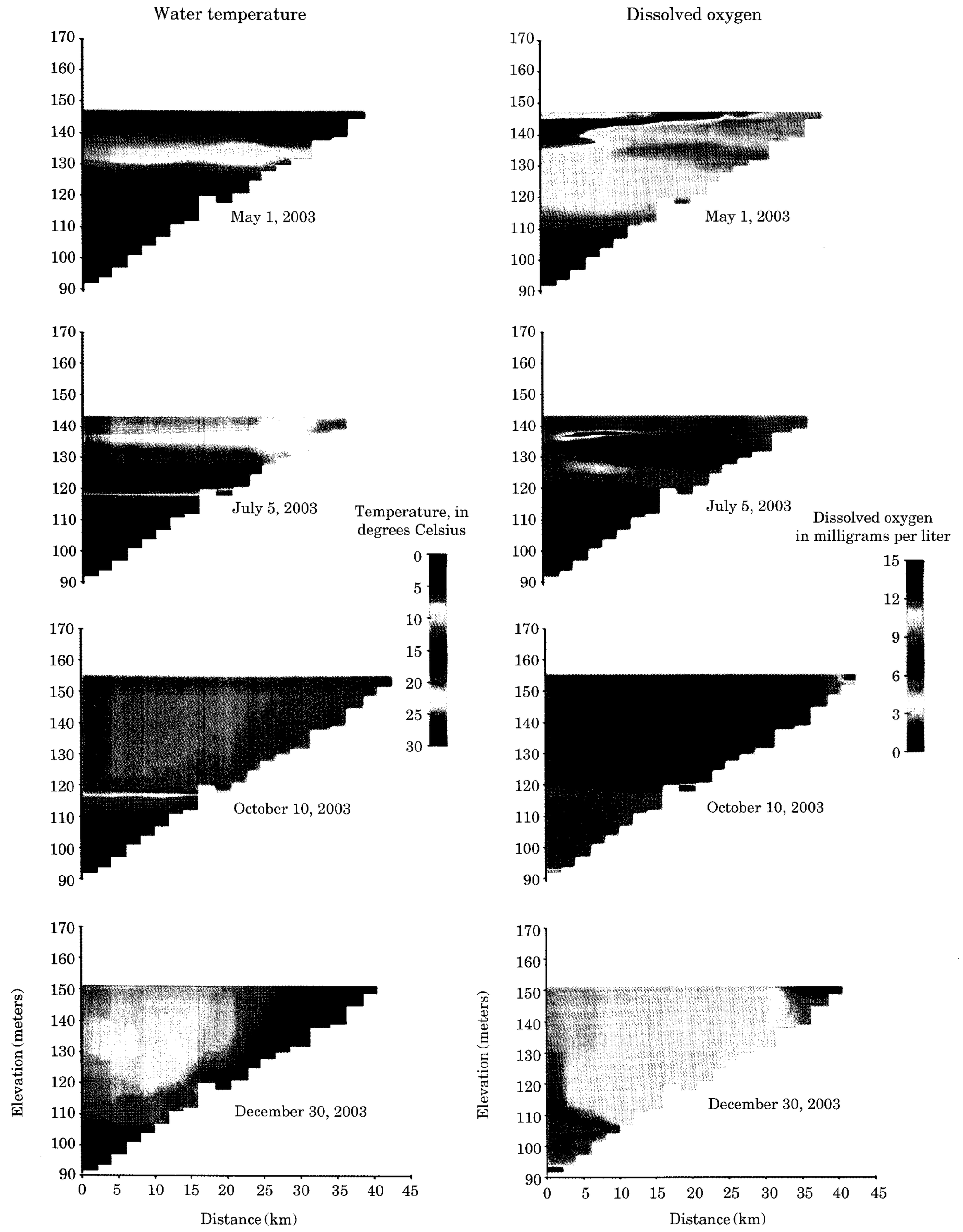

Fig. 15. Longitudinal slices through model grid showing modeled temperature and dissolved oxygen in Andong Reservoir on selected dates in 2003, to illustrate the typical seasonal patterns that occur in the reservoir.

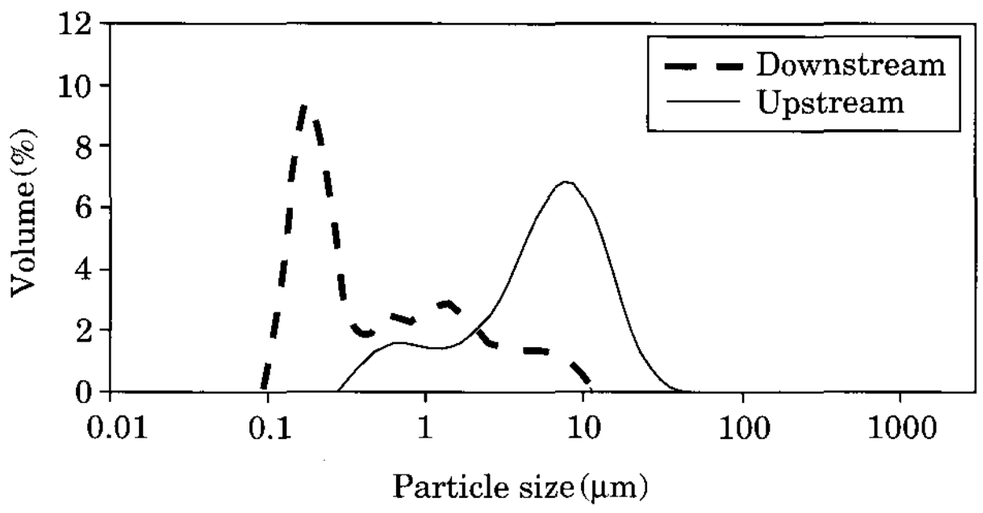

Fig. 16. Particle size distribution of suspended particles.

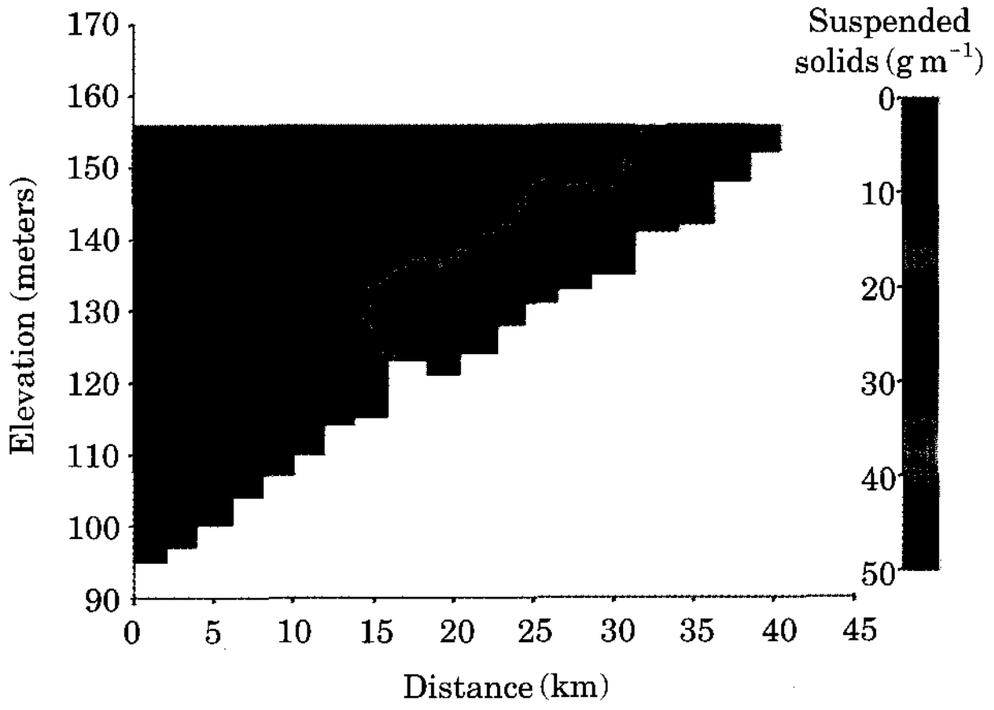

Fig. 18. Plot of Suspended Solids on 12th September, 2003.

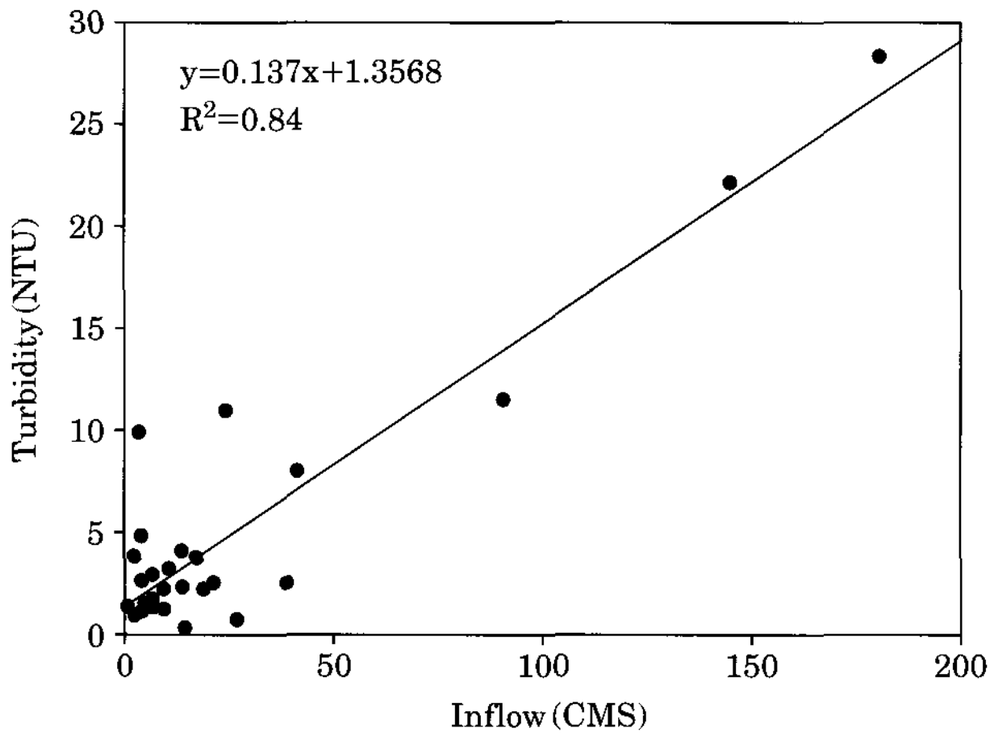

Fig. 17. Plot of inflow rate and turbidity.

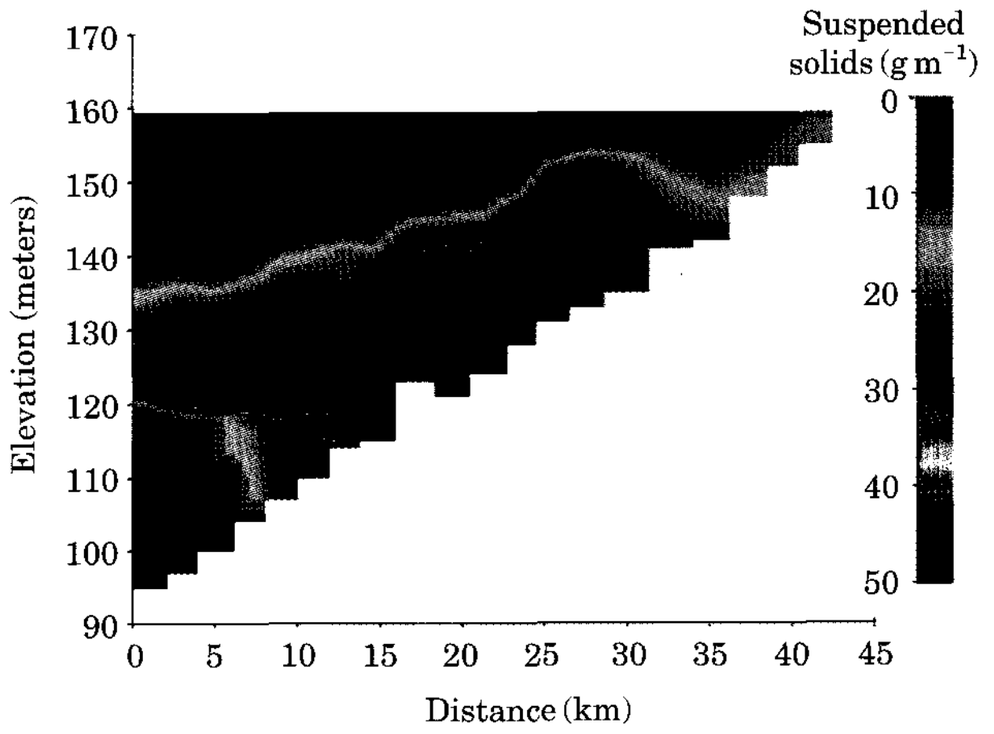

Fig. 19. Plot of Suspended Solids on 16th September, 2003.

rates and greater contributions by coarser sediments (Pemberton and Blanton, 1980) in riverine and transition zones of reservoirs.

The particulate size distribution of turbid water showed that most of the larger and heavier particles in the size near 10 μm were dominant in the inflowing stream, and the finer ones of less than 1 μm in size remained in suspension and were longitudinally transported to the main section of the dam (Fig. 16). These lighter particles have a very low settling rate and thus have a significant effect on the water column nutrient dynamics as well as on the biological stock (Kennedy and Walker, 1990). Due to the lack of sufficient data on suspended solids, it was calculated from the relationship derived from the correlation of inflow rate (Q) and turbidity (NTU) which showed a strong positive linear relationship with the R^2 value of 0.84 (Fig. 17).

As, the CE-QUAL-W2 model is based on the assumption of lateral homogeneity, the suspended solids concentration results are uniform in the lateral direction. But, in reality the concentrations generally decrease with distance away from the dominant flow path (Kim, 2005). In the Andong Reservoir model, the inorganic suspended solids were grouped according to the inflow rate of: a) <100 CMS day^{-1}, and b) >100 CMS day^{-1}. This allowed us to assign settling velocity of 0.1 m day^{-1} and 0.9 m day^{-1} for each group of suspended solids, respectively.

The phenomenon of onset of reservoir density current, movement of density front and formation of interflow were vividly simulated in this study. The observation data from September 12 and September 16, 2003, were used to calibrate density flows within the reservoir as around this period of the year substantial inflows were recorded. The spatial and temporal transportation

patterns of density flow for those dates are shown in the Fig. 18 and Fig. 19, respectively. On 12th September, 2003, the turbid flow had taken the shape of the underflow and was flowing along the bed of the riverine slope of the Andong Reservoir (Fig. 18). Just after four days, the head of the turbid flow clearly formed the interflow and was steadily moving towards the dam outlet with the thickness of about 15 m (Fig. 19). Also, notice the increase in the surface water level [given as elevation (m) on left hand side]. On the sampling date of 10th October, almost a month later, the metalimnion had still a very high turbidity concentration of 120 (NTU) at the depth of 30 m.

CONCLUSION AND SUMMARY

The CE-QUAL-W2 model [Version 3.2], a two dimensional, longitudinal/vertical, hydrodynamic, and water quality model (Cole and Wells, 2003) was applied to model the Andong Reservoir to understand the underlying hydrological and water quality issues.

The hydrodynamic model was calibrated for the year of 2003 and verified with single continuous run from 2000~2004. The model boundaries on the Andong Reservoir extended from inflowing river up to the Andong Reservoir. The hydrodynamic model extremely well simulated the large and rapid changes in the surface water level brought by the seasonal storm runoff. Accurate and precise bathymetry data were the most important factors affecting the ability to reduce the model surface water level error. The model also successfully reproduced the temporal and spatial distribution of temperature and thermodynamical behaviors, starting the year cold and isothermal, the reservoir developed a thermocline by early summer, and turning over in the winter. This hydro-thermal characteristic of Andong Reservoir is also shared by other deep watered reservoirs located in the temperate region. The mixing pattern as well as the descending thermocline, onset and duration of stratification and timing of turnover phenomenon were also well reproduced by the Andong Model. The model may thus be used to evaluate management issues concerning the stratification and mixing regimes of Andong Reservoir. The temperature model predictions were very dependent on upstream boundary conditions as evidenced by short travel times, discharge gate location and inflow temperature. The accurate spatial and temporal distribution of temperatures in Andong Reservoir lays a strong foundation to the water quality model, as many kinetic processes in the water column are temperature dependent. As suggested in the CE-QUAL-W2 manual, the hydrodynamic model was further improved with the modeling of dissolved oxygen. The model performed well in simulating not only the dissolved oxygen profiles but, also it was able to mimic the metalimnetic dissolved minima phenomenon, which is a commonly occurring phenomenon in stratified deep reservoirs of temperate regions. Boundary conditions, algae growth rates, respiration and photosynthesis rate, reaeration equation and sediment oxygen demand were particularly important for model calibration. The depth-distance profile showed that the metalimnion layer had high turbid contents during the period of metalimnetic dissolved oxygen minima and also the same period coincided with the growing algal season. This further sheds some light on the complex nature of dissolved oxygen distribution in Andong Reservoir. The calibrated model well simulated the formation and interflow of density current in Andong Reservoir, another characteristics of other large reservoirs located in the Asian summer monsoon region. The differences in the settling velocity of the suspended solids arising due to the size sorting processes were particularly important in the modeling effort.

This effective application of hydro-thermal module of CE-QUAL-W2 model in Andong Reservoir serve as a strong basis for future application of water quality models in Andong Reservoir, and evaluate different "what-if" management scenarios. With the future collection of more site specific data, this model can be improved to get an in-depth understanding of various complex processes at play and analyze the factors affecting them.

ACKNOWLEDGEMENT

This work was supported by the Korea Research Foundation Grant funded by the Korean Government (MOEHRD, Basic Research Promotion Fund) (KRF-2006-211-D500085).

LITERATURE CITED

Alavian, V., G.H. Jirka, R.A. Denton, M.C. Johnson and H.G. Stefan. 1992. Density currents entering Lakes and Reservoirs. *J. of Hydr. Engl.* **118**(11): 1464-1489.

An, K-G. 2000. Dynamic changes of dissolved oxygen during summer monsoon. *Korean J. Limnol.* **33**: 213-221.

Buchak, E.M. and J.E. Edinger. 1982. User guide for LARM2: A longitudinal-vertical, time-varying hydrodynamic reservoir model. Instructional Report E-82-3, US Army Engineer Waterways Experiment Station, Vicksburg, MS.

Chung, S.W. and R. Gu. 1998. Two-dimensional simulations of contaminant currents in stratified reservoir. *J. Hydraul. Eng.* **124**(7): 704-711.

Cole, T. and E. Buchak. 1995. CE-QUAL-W2: A two-dimensional, laterally averaged, hydrodynamic and water quality model, Version 2.0, Technical Report El-95-1, U.S. Army Engineer Waterways Experiment Station, Vicksburg, MS.

Cole, Thomas M. and Dorothy H. Tillman. 1997. Water quality Modeling of Lake Monroe using CE-QUAL-W2. Miscellaneous Paper EL-99-1, US Army Engineer Waterways Experiment Station, Vicksburg, MS.

Cole, T.M. and H.H. Hannan. 1990. Dissolved oxygen dynamics in Thornton, K.W., Kimmel, B.L. and Payne, F., Reservoir Limnology: Ecological Perspectives. John Wiley and Sons, Inc. Chapter 4, p. 71-107.

Cole, T.M. and S.A. Wells. 2003. CE-QUAL-W2: A two-dimensional, laterally averaged, hydrodynamic and water quality model, Version 3.2. Instruction Report EL-03-1, US Army Engineering and Research Development Center, Vicksburg, MS.

Dirnberger, J.M. and S.T. Threlkeld. 1986. Advective effects on reservoir zooplankton dispersion and abundance. *Freshwat. Biol.* **16**: 387-396.

Effler, S.W. and D.A. Matthews. 2004. Sediment resuspension and drawdown in a water supply reservoir. *J. Am. Water Resour. Assoc.* **40**: 251-264.

Effler, S.W., C.M. Matthews (Brooks) and D.A. Matthews. 2001. Patterns of gross deposition in reservoirs enriched in inorganic tripton. *Can. J. Fish. Aquat. Sci.* **58**: 2177-2188.

Gibson, C.E. and J. Guillot. 1997. Sedimentation in a large lake: the importance of fluctuations in water level. *Freshwat. Biol.* **37**: 597-604.

Gloss, S.P., L.M. Mayer and D.E. Kidd. 1980. Advective control of nutrient dynamics in the epilimnion of a large reservoir. *Limnol. Oceanogr.* **25**: 219-228.

Heo, W.M., B. Kim, Y. Kim and K.S. Cho. 1998. Storm runoff of phosphorus from non-point sources into Lake Soyang and transportation of turbid water mass within the lake. *Kor. J. Lim.* **31**(1): 1-8.

Hutchinson, G.C. 1957. A treatise on limnology. Vol. 1. Geography, physics and chemistry. John Wiley and Sons, NY.

Jiahua, F. 1986. Turbidity density currents in reservoirs. *Water Int.* **11**: 107-116.

Kennedy, R.H. and W.W. Walker. 1990. Reservoir nutrient dynamics. In: Thornton, K.W., *et al.* (Eds.), Reservoir Limnology: Ecological Perspectives. John Wiley and Sons, New York, p. 109-132, Chapter 5.

Kim, Y. 2005. Dynamics of phosphorus in a deep reservoir, Lake Soyang, in Asian Monsoon Area. Ph. D. Thesis. Kangwon National University, Korea.

Kim, Y. and B. Kim. 2006. Application of a 2-dimensional water quality model (CE-QUAL-W2) to the turbidity interflow in a deep reservoir (Lake Soyang, Korea). *Lake and Reserv. Manage.* **22**(3): 213-222.

Korea Water Resources Corporation (KWATER). 1996. Annual report of management of Lake Andong.

Korea Water Resources Corporation (KWATER). 2005. Annual report of management of Lake Andong.

Korea Water Resources Corporation (KWATER). 2006. Annual report of management of Lake Andong.

Korean Meteorological Association. 2004. Annual report.

Laenen, A. and A.P. LeTourneau. 1996. Upper Klamath Basin nutrient loading study-estimate of wind-induced re-suspension of bed sediment during periods of low lake elevation. USGS Open-File Report, p. 95-414.

Lind, O.T., R. Doyle, D.S. Vodopich, B.G. Trotter, J. G. Limon and L. Davalos-Lind. 1992. Clay turbidity: Regulation of phytoplankton production in a large, nutrient-rich tropical lake. *Limnol. Oceanogr.* **37**: 549-565.

Orlob, G.T. 1983. Mathematical modeling of water quality: Streams, Lakes, and Reservoirs. International Series on Applied System Analysis, Vol. 12, John Wiley & Sons, New York.

Park, J.C., W.P. Jung and J.K. Shin. 2006. The cause of Metalimnetic DO Minima in Andong Reservoir, Korea. *Kor. J. Limnol.* **39**: 112

Pemberton, E.L. and J.O. Blanton III. 1980. Procedure for monitoring reservoir sedimentation. Proc., Symp. Surface Water Impoundments. ASCE, New York, p. 1269-1278.

Soltero, R.A., A.F. Gasperino and W.G. Graham. 1974. Chemical and physical characteristics of a eutrophic reservoir and its tributaries: Long Lake, Washington. *Wat. Res.* **8**: 419-431.

Thomann, R.V. 1982. Verification of water quality models. *J. Environ. Eng. ASCE* **108**: 723-940.

Walker, W.W. 1987. Empirical methods of predicting eutrophication in impoundments. Report 4: Phase

III: Applications manual Technical report E-81-9. US Army Waterways Experimental Station. Vicksburg, MS.

Wetzel, R.G. 1983. Limnology. Saunders Publishing, Philadelphia, PA.

Wunderlich, W.O. 1971. The dynamics of density-stratified reservoirs. p. 219-231 in G.E. Hall, ed. Reservoir, fisheries and Limnology. Spec. Pub. 8th *Amer. Fish Soc.* Washington, DC.

(Manuscript received 18 February 2008,
Revision accepted 24 March 2008)